Exploring the Limitations of the Convolutional Neural Networks on Binary Tests Selection for Local Features

Bernardo Janko Gonçalves Biesseck[1,2], Edson Roteia Araujo Junior[1] and Erickson R. Nascimento[1]
[1] *Universidade Federal de Minas Gerais (UFMG), Brazil*
[2] *Instituto Federal de Mato Grosso (IFMT), Brazil*

Keywords: Binary Tests, Keypoint Descriptor, Convolutional Neural Network.

Abstract: Convolutional Neural Networks (CNN) have been successfully used to recognize and extract visual patterns in different tasks such as object detection, object classification, scene recognition, and image retrieval. The CNNs have also contributed in local features extraction by learning local representations. A representative approach is LIFT that generates keypoint descriptors more discriminative than handcrafted algorithms like SIFT, BRIEF, and SURF. In this paper, we investigate the binary tests selection problem, and we present an in-depth study of the limit of searching solutions with CNNs when the gradient is computed from the local neighborhood of the selected pixels. We performed several experiments with a Siamese Network trained with corresponding and non-corresponding patch pairs. Our results show the presence of *Local Minima* and also a problem that we called *Incorrect Gradient Components*. We pursued to understand the binary tests selection problem and even some limitations of Convolutional Neural Networks to avoid searching for solutions in unviable directions.

1 INTRODUCTION

Local floating point descriptors, such as SIFT (Lowe, 2004), SURF (Bay et al., 2006), and HOG (Dalal and Triggs, 2005), are well known in literature as being discriminative and robust to rotation, scale, and illumination changes in images. However, they have a high computational cost and are expensive to store, which make difficult running these float descriptors on computers with limited hardware (e.g., embedded systems, smartphones, etc.) when the number of images and descriptors are large.

A popular approach to reduce computational cost is to design a local feature extractor that creates binary descriptors. Designed to be fast, binary descriptors are based on binary tests that compare pixels intensities around a keypoint. While each SIFT descriptor occupies 512 bytes of memory and uses the Euclidean distance as a similarity measure, a BRIEF (Calonder et al., 2010) descriptor, for instance, needs 32 Bytes and uses Hamming distance to compare two feature vectors.

The past decade has witnessed an explosion of similar approaches to BRIEF, each one using a different binary tests set. ORB (Rublee et al., 2011), BRISK (Leutenegger et al., 2011) and FREAK (Ortiz, 2012) are three descriptors that explore different image properties and spatial pattern of binary tests to improve their robustness and matching performance. Recently, binary descriptors based on Convolutional Neural Networks (CNN) have been created, such as DeepBit (Lin et al., 2016) and DBD-MQ (Duan et al., 2017). However, these CNN-based methods still have high computational cost because of the several layers of the deep networks used on their solutions.

Virtually all binary descriptors define a spatial pattern to be used to select the pixels when extracting the local features. Beyond being a common step on binary descriptors, the spatial pattern is crucial for the matching performance. Motivated to discovering new patterns of binary tests, we propose to answer the following question: *Is a CNN-based model able to find a spatial distribution of binary test that minimizes distances between corresponding keypoints and maximizes distances between non-corresponding keypoints?* Our idea is to use the CNN power to extract distributions not yet observed by the scientific community. Our results demonstrate two significant hindrances to the use of CNN on binary tests selections: the existence of *Local Minima* and what we called *Incorrect Gradient Components*. These two problems appear when the objective function gradient (used in the

Biesseck, B., Araujo Junior, E. and Nascimento, E.
Exploring the Limitations of the Convolutional Neural Networks on Binary Tests Selection for Local Features.
DOI: 10.5220/0007374102610271
In *Proceedings of the 14th International Joint Conference on Computer Vision, Imaging and Computer Graphics Theory and Applications (VISIGRAPP 2019)*, pages 261-271
ISBN: 978-989-758-354-4

Back-propagation step) is calculated from the local pixel's neighborhood. As main contribution, we present in this paper some limitations of CNN in binary tests selection to understand the robustness and the limits of using CNNs on binary tests selection for local feature extraction.

2 RELATED WORK

Binary descriptors have been presented as alternative approaches to floating point descriptors. They are useful mainly in applications running on computers with limited resources, such as embedded systems, smartphones, etc. A binary descriptor is composed of bits that are, in general, the result of binary tests defined as

$$\tau(I,x,y,w,z) = \begin{cases} 1 & \text{if } I(x,y) < I(w,z), \\ 0 & \text{otherwise,} \end{cases} \tag{1}$$

where $I(x,y)$ and $I(w,z)$ are the intensities of pixels (x,y) and (w,z) of a digital image I. Each binary test compares two pixels and a set of n binary tests compose a binary descriptor.

A patch of size 31×31 has $M = \binom{N}{2} = 461{,}280$ different binary tests considering all $N = 961$ pixels. Using all of them it is impractical, it would take $M/8 = 57{,}660$ Bytes to store only one descriptor. Therefore, choosing a small set of binary tests is important to keep descriptor compact and fast.

BRIEF (Calonder et al., 2010) is a popularone of the most popular keypoint binary descriptors, whose binary tests selection is performed randomly using a Normal distribution around the keypoint. Although BRIEF is not invariant to rotation, it demonstrated that even patches could be described in a simple way and fair discriminative representation. Figure 1-a shows a visualization of the selected binary tests of the BRIEF descriptor. ORB (Rublee et al., 2011) is an extension of BRIEF, but its binary tests selections were developed from statistical properties. Instead of a random selection, the authors used a greedy search to select the 256 binary tests with higher variance and lower correlation, what improved its discrimination power. Figure 1-b shows a visualization of the ORB binary tests.

BRISK (Leutenegger et al., 2011) and FREAK (Ortiz, 2012) are based on fixed sets of points, defined by their designers. The BRISK's binary tests are organized using 60 concentric points, as shown in Figure 1-c, from which two sets of binary tests are created: L (long-distance) and S (short-distance). L set is used to compute canonical orientation and the S set,

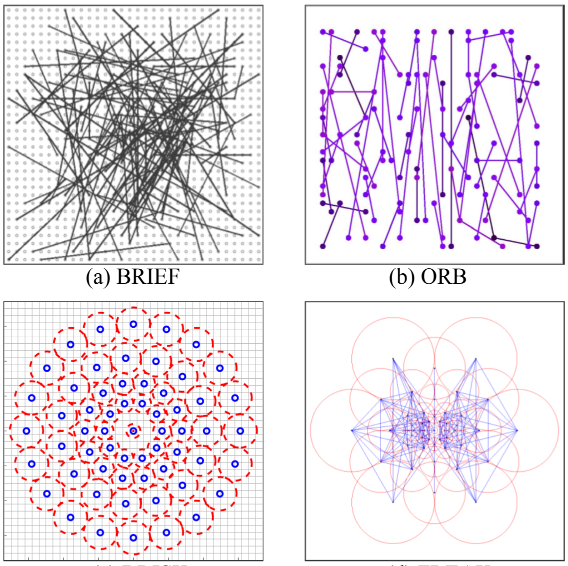

(a) BRIEF (b) ORB (c) BRISK (d) FREAK

Figure 1: Different spatial distribution used to extract binary tests: a) BRIEF (Calonder et al., 2010); b) ORB (Rublee et al., 2011); c) BRISK (Leutenegger et al., 2011); and d) FREAK (Ortiz, 2012). Images extracted from the original papers.

containing 512 binary tests, is used to generate the final descriptor. FREAK's binary tests, for their turn, are based on the human eye, more specifically on human retina, where light receptor cells concentration is higher in the central region. From the 43 points and $\binom{43}{2} = 903$ possible pairs, 512 binary tests were selected like ORB greedy search. Figure 1-d shows the locations of the points and final binary tests used by FREAK.

Instead of using only pixel intensity, the OSRI descriptor (Xu et al., 2014) is generated by comparing invariant to rotation and illumination subregions, which are defined according to pixels intensities and gradients orientation. To build the final binary vector, the best bits are selected by a cascade filter. BOLD descriptors (Balntas et al., 2015) select the best binary tests by a global and local optimization process. The global optimization is performed offline, and it identifies the binary tests with high variance and low correlation in a total set of N patches. In the local optimization, each patch is considered a separate class and new synthetic instances are generated online to estimate intra-class variance. This second step selects the binary tests that minimize the variance.

Most recently, binary descriptors based on Convolutional Neural Networks (CNN) are being used in local feature extraction. Two representative approaches are the DeepBit (Lin et al., 2016) and DBD-MQ (Duan et al., 2017). They use the 16 pre-trained layers of VGG network (Simonyan and Zisserman, 2015) that is fine-tuned by matching local regions using corresponding and non-corresponding patch pairs. In these works, there is no an exact definition of the binary tests coordinates, since their general idea is to learn weights that minimize the quantization error of the real output vector to bits 0 and 1. Despite the quality of their results, binarizing the last layer maintains a high computational cost. In this paper, we evaluated CNN ability in binary tests selection, aiming to discovery different spatial distributions to create discriminant descriptors.

3 METHODOLOGY

3.1 Convolutional Neural Network

Based on the Network proposed by (Simo-Serra et al., 2015), we built a Convolutional Neural Network with 4 layers. The first three layers consist of blocks of convolution, pooling and activation function, and the last layer is fully connected that outputs the coordinates θ_i of binary tests for each patch p_i.

The first layer contains 32 convolution kernels of size 7×7, followed by a 2×2 max pooling window and activation function *tanh*. The second layer is composed of 64 convolution kernels 6×6, followed by a 3×3 max pooling window and activation *tanh*. In the third layer, we used 128 convolution kernels 5×5, a 4×4 max pooling window and activation function *tanh*. The fourth layer has no convolution neither pooling, but only the weights of each processing unit and the activation function *sigmoid*. The activation function is applied to limit the output inside the interval $(0,1)$, which allows to scale easily to the interval $[0,S]$ multiplying θ_i by S, where $S\times S$ is the size of a training patch p_i. Figure 2 shows a visualization of the CNN structure. The final network contains a total of $805,632$ parameters.

To learn the binary tests, we created a Siamese Network using 2 CNNs with the aforementioned architecture. They share all weights W_i and bias b_i, allowing to train them with patch pairs. Figure 2 illustrates the architecture. Since we aim to minimize the distance between corresponding and maximize the distances between non-corresponding patch descriptors, we added the layers $d_i(p_i,\theta_i)$, $H(d_1,d_2)$ and $L(H,y)$ to the Siamese Network. Layer $d_i(p_i,\theta_i)$ computes the binary descriptor from the coordinates θ_i generated by patch p_i. $H(d_1,d_2)$ calculates the Hamming distance between the descriptors d_1 and d_2. Finally, $L(H,y)$ computes the error using $ContrastiveLoss$ function (Simo-Serra et al., 2015),

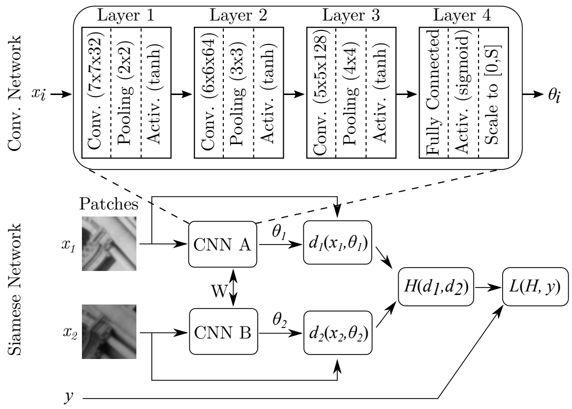

Figure 2: Convolutional Network and Siamese Network architectures. The Siamese Network is composed of 2 Convolutional Networks that share W_i and b_i weights and support the processing of *patches* pairs. For each *patch* p_i, a coordinates vector θ_i is generated.

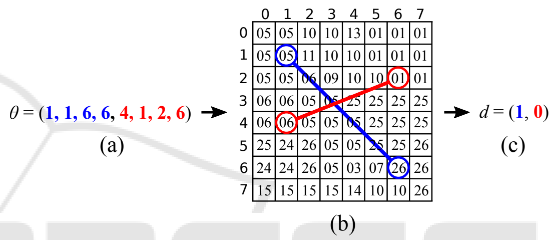

Figure 3: Representation of the θ vector for a 2-bits binary descriptor d. a) An instance of the θ vector, $\theta \in \mathbb{N}^8$. b) Binary tests visualization on a 8×8 patch. c) Resulting binary descriptor d from pixel intensities comparison of the binary tests.

defined as

$$L(H,y) = \begin{cases} H^2 & \text{if } y = 1, \\ \max(0, C-H)^2 & \text{if } y = 0, \end{cases} \tag{2}$$

where $y \in \{1,0\}$ is a binary variable that defines if a patch pair is corresponding (1) or non-corresponding (0). Equation 2 can be rewritten as

$$L(H,y) = y \cdot H^2 + (1-y) \cdot \max(0, C-H)^2 \tag{3}$$

for implementation convenience. The C constant defines the minimum H distance for descriptors of non-corresponding patches, penalizing smaller values. In contrast, the distances between corresponding patches should be minimized to 0.

3.2 Binary Tests

Given a patch p_i of size $S\times S$ extracted from a digital image I, a binary test $\tau(p_i,x,y,w,z)$ is a function that compares pixels $p_i(x,y)$ and $p_i(w,z)$ intensities. Therefore, 4 coordinates are required for each binary test. To represent a binary descriptor d with n bits, the fourth layer of each CNN has been configured to provide a vector $\theta_i \in \mathbb{N}^4$, where $0 \leq \theta_i \leq S$. Figure 3 illustrates an instance of θ for a 2-bits binary descriptor. The coordinates $(1,1,6,6)$ form the first binary test, whose result is 1 because pixel intensity $p_i(1,1) = 05$ is less than pixel intensity $p_i(6,6) = 26$ and, likewise, the coordinates $(4,1,2,6)$ of second binary test results in 0 because $p_i(4,1) = 06$ is not less than $p_i(2,6) = 01$.

3.3 Gradient

The back-propagation algorithm, used to to update the weights W_i and b_i, depends on the gradient $\nabla_i L = \left\{\frac{\partial L}{\partial W_i}, \frac{\partial L}{\partial b_i}\right\}$ of loss function L. Since a Neural Network is a composite function, it is possible to calculate its gradients using the chain rule by equations

$$\frac{\partial L}{\partial W_i} = \frac{\partial L}{\partial H}\left(\frac{\partial H}{\partial d_1}\frac{\partial d_1}{\partial \theta_1}\frac{\partial \theta_1}{\partial W_i} + \frac{\partial H}{\partial d_2}\frac{\partial d_2}{\partial \theta_2}\frac{\partial \theta_2}{\partial W_i}\right) \tag{4}$$

and

$$\frac{\partial L}{\partial b_i} = \frac{\partial L}{\partial H}\left(\frac{\partial H}{\partial d_1}\frac{\partial d_1}{\partial \theta_1}\frac{\partial \theta_1}{\partial b_i} + \frac{\partial H}{\partial d_2}\frac{\partial d_2}{\partial \theta_2}\frac{\partial \theta_2}{\partial b_i}\right). \tag{5}$$

Each training patch pair provides a partial derivative $\frac{\partial L}{\partial H}$ indicating the direction to modify the Hamming distance and reduce total error. For corresponding patches $\frac{\partial L}{\partial H} > 0$ when $H(d_1,d_2) > 0$, what means the Hamming distance must decrease. For non-corresponding patches $\frac{\partial L}{\partial H} < 0$ when $H(d_1,d_2) < C$, indicating that the network must try to increase the distance to be greater than C. In the previous layer, the derivatives $\frac{\partial H}{\partial d_1}$ and $\frac{\partial H}{\partial d_2}$ indicate which bits of current binary descriptors d_1 and d_2 must be modified to follow the direction indicated by $\frac{\partial L}{\partial H}$. Likewise, the derivatives $\frac{\partial d_1}{\partial \theta_1}$ and $\frac{\partial d_2}{\partial \theta_2}$ indicate the directions to change binary tests coordinates θ_1 and θ_2 to modify the bits indicated by $\frac{\partial H}{\partial d_1}$ and $\frac{\partial H}{\partial d_2}$. Furthermore, the derivatives $\frac{\partial \theta_1}{\partial W_i}$, $\frac{\partial \theta_2}{\partial W_i}$, $\frac{\partial \theta_1}{\partial b_i}$ and $\frac{\partial \theta_2}{\partial b_i}$ indicate the updating directions of the W_i and b_i weights so that the pixels indicated by $\frac{\partial d_1}{\partial \theta_1}$ and $\frac{\partial d_2}{\partial \theta_2}$ are selected.

Partial derivatives $\frac{\partial L}{\partial H}$ and $\frac{\partial \theta_i}{\partial W_i}$ can be calculated analytically but $\frac{\partial H}{\partial d_i}$ and $\frac{\partial d_i}{\partial \theta_i}$ cannot because they depend on non-differentiable operations, such as *Exclusive OR* and pixels intensities comparison. Thus, we approximate $\frac{\partial L}{\partial \theta_i}$ numerically by finite differences as follows. First we define

$$L_1^+ = L(H(d_1(x_1,\theta_1+\Delta), d_2(x_2,\theta_2)), y), \tag{6}$$

$$L_1^- = L(H(d_1(x_1,\theta_1-\Delta), d_2(x_2,\theta_2)), y), \tag{7}$$

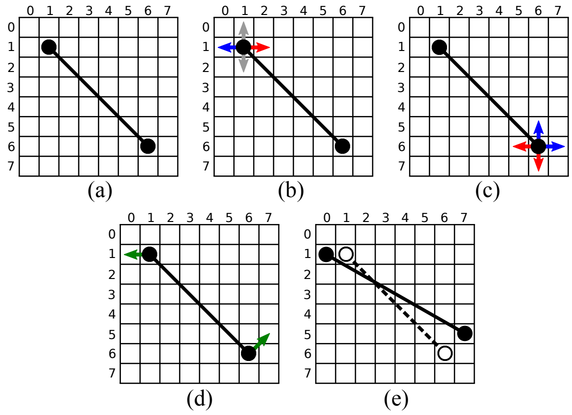

Figure 4: Illustration of binary tests selection process. a) One binary test $\theta = (x_1, y_1, x_2, y_2)$ on a patch of size 8×8; b) and c) the error on horizontal e vertical directions when changing coordinates x_1, y_1, x_2 and y_2. Blue arrows indicate the error decreases, red arrows indicate the error increases and gray arrows indicate the error does not change. d) Green arrows indicate the resulting directions when changing coordinates x_1, y_1, x_2 and y_2 after error computation; e) Resulting binary test after updating network weights.

$$L_2^+ = L(H(d_1(x_1,\theta_1), d_2(x_2,\theta_2+\Delta)), y), \tag{8}$$

$$L_2^- = L(H(d_1(x_1,\theta_1), d_2(x_2,\theta_2-\Delta)), y), \tag{9}$$

then, using the centralized formula we obtain

$$\frac{\partial L}{\partial \theta_1} = \frac{L_1^+ - L_1^-}{2\delta}, \tag{10}$$

$$\frac{\partial L}{\partial \theta_1} = \frac{L_2^+ - L_2^-}{2\delta}. \tag{11}$$

In terms of pixels coordinates, we have $\min \delta = 1$ for the original image resolution and $\Delta = (\delta_1, \delta_2, \ldots, \delta_N)$, where $\delta_i = 1$ and $N = 4 \cdot \#bits$. Thus, the gradients $\frac{\partial L}{\partial W_i}$ and $\frac{\partial L}{\partial b_i}$ were calculated as

$$\frac{\partial L}{\partial W_i} = \frac{\partial L}{\partial \theta_1}\frac{\partial \theta_1}{\partial W_i} + \frac{\partial L}{\partial \theta_2}\frac{\partial \theta_2}{\partial W_i}, \tag{12}$$

$$\frac{\partial L}{\partial b_i} = \frac{\partial L}{\partial \theta_1}\frac{\partial \theta_1}{\partial b_i} + \frac{\partial L}{\partial \theta_2}\frac{\partial \theta_2}{\partial b_i} \tag{13}$$

instead of using Equations 4 and 5.

Applying this formulation, the Siamese Network changes the pixels coordinates in horizontal and vertical directions to choose binary tests that decrease the total error. This is done by selecting binary tests that reduces the Hamming distance between descriptors of the corresponding patch pairs and increase the Hamming distance between non-corresponding pairs. Figure 4 illustrates the coordinates variation process and the resulting binary test.

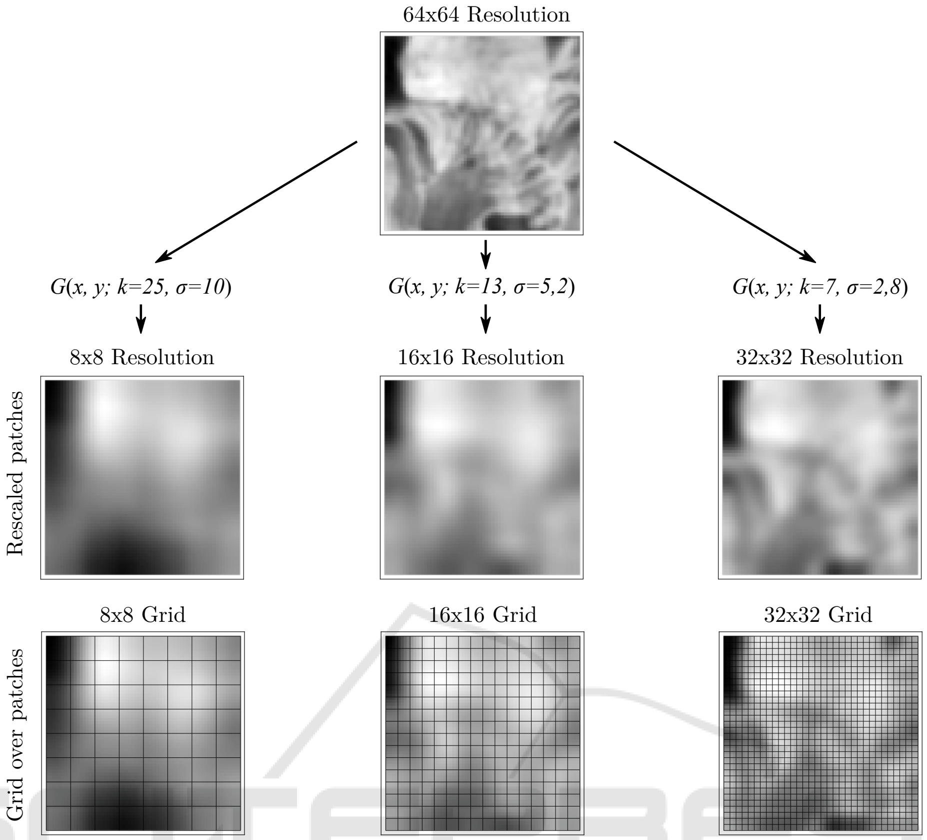

Figure 5: Patch 64×64 rescaled with Gaussian filters $G(x, y; k, \sigma)$ to 8×8, 16×16 and 32×32 resolutions. A $r \times r$ grid corresponding to the current resolution r is applied to ensure the spatial distribution of the binary tests over the rescaled patches. In this case, binary tests can be composed of only the central pixels of each grid block.

3.4 Multiscale Trainning

After running experiments using binary tests representation described in subsection 3.2 and the numerical approximation of gradients $\frac{\partial L}{\partial \theta_1}$ and $\frac{\partial L}{\partial \theta_2}$, we discovered that the Siamese Network reached local minimum during training. This local minimum enforces the network to stop learning before the error becomes satisfactorily low. Section 4 presents the details and thorough analysis of the local minimum problem.

To reduce the impacts of local minimum, we trained the network using image pyramid, from lowest resolution to highest. This approach allows the Siamese Network to view whole patches and select discriminative regions before choosing specific binary tests. Scale reduction was performed by applying convolutions with a Gaussian filter

$$G(x, y; k, \sigma) = \frac{1}{2\pi\sigma^2} e^{-\frac{x^2+y^2}{2\sigma^2}}, \tag{14}$$

where $k \times k$ are the dimensions of kernel, computed as $k = \left(\frac{3S}{r} + 1\right)$, $S \times S$ the dimensions of patch, r the spatial resolution for which patches will be reduced and $\sigma = \frac{k}{f}$. In our experiments, we used $f = 2.5$ to cover 98.76% of Gaussian kernel.

4 EXPERIMENTS

We performed several experiments to evaluate the network behavior when selecting the binary tests. We used patches of 64×64 size extracted from the dataset Trevi Fountain (Winder and Brown, 2007) to compose corresponding and non-matching pairs. The Trevi Fountain dataset contains more than 30,000 keypoints, each one containing between 5 and 50 instances (patches) captured under rotation, scale, and illumination changes.

To improve the generalization capacity, we enforced an uniform selection of patches by assigning to each keypoint the quotas $Q_{cp} = \lceil P \cdot \frac{T}{k} \rceil$ of corresponding pairs and $Q_{np} = \lfloor N \cdot \frac{T}{k} \rfloor$ of non-matching pairs. These quotas are based on total amount T of patch pairs to be created, k amount of available keypoints for trainning and on desired percentages $P \in [0, 1]$ and

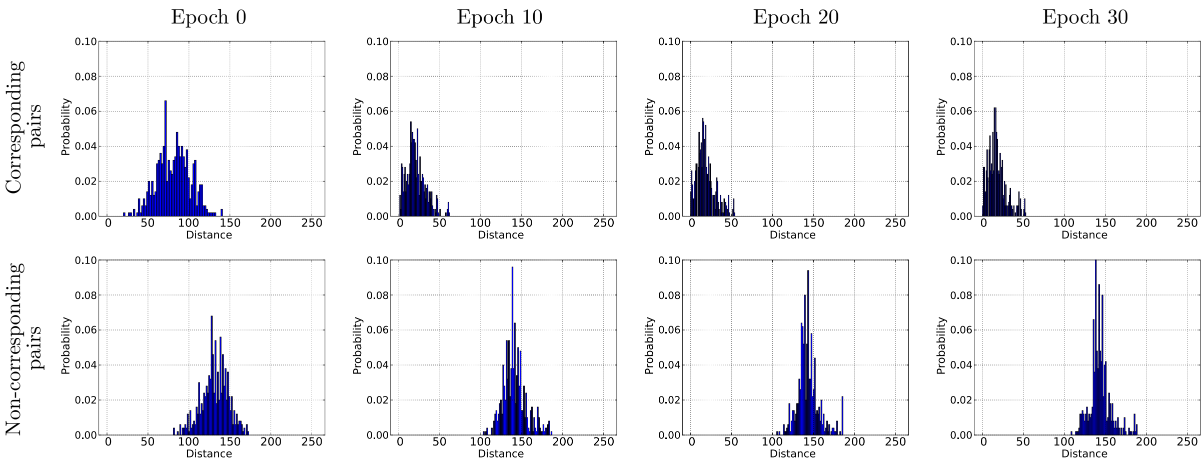

Figure 6: Distribution of distances between correspondent and non-correspondent pairs during Siamese Network Training. The results of Epoch 0 are before the beginning of the training phase, with random W_i and b_i weights. One can clearly see that the distances of the correspondent pairs decreased over the training, while non-correspondent distances concentrate around the 125 value. This behavior demonstrates the correct learning of the binary tests.

$N = 1 - P$ of corresponding and non-corresponding pairs, respectively. Thus, at least two patches of each keypoint are used.

The siamese network was trained using the K-Fold protocol, with $K = 5$. Three folds were used for training, one for validation and one for testing. We created $T = 10{,}000$ patch pairs per fold, where 50% were corresponding and 50% non-corresponding pairs. The network was trained with a total of $30{,}000$ pairs. For optimization we used the Stochastic Gradient Descent (SGD) algorithm, with batch size 32, learning rate 1×10^{-9}, momentum 0.9 and decay 1×10^{-3}. We performed 30 training epochs because decreasing error rate stagnates after this value. In objective function, i.e., contrastive loss, the best result was obtained using margin $C = 150$. Our model were implemented in Python with Keras (Chollet et al., 2015) and Theano (Theano Development Team, 2016) libraries.

4.1 Distances Distributions

The distance distributions indicate whether network learning of binary tests is occurring as expected. Ideally, distances between corresponding patch descriptors should be close to zero, and distances between non-corresponding descriptors should be large, according to the applied similarity measure.

We performed this analysis observing distances every 10 training epochs, where epoch 0 refers to the initial state of Siamese Network, with weights randomly initialized. Figure 6 presents the histograms of distances that demonstrate the expected behavior because the distances between corresponding patch descriptors were reduced while the distances between non-corresponding descriptors increased during training. In the first row, one can observe distances between corresponding patch descriptors moving to the left side while distances between non-corresponding patch descriptors go to the right side and stop around 150.

4.2 Local Minima

Binary tests selection based on the local pixel's neighborhood is limited by Local Minima problem due to the spatial distribution of pixels intensities. At the beginning of the training step, until epoch 10, horizontal and vertical variations of coordinates θ_i reduce the error, but after some epochs, the immediate neighbors $\theta_i + \Delta$ and $\theta_i - \Delta$ do not change order relation between pixels of the current binary tests. It means the resulting bits remain the same when the network change coordinates in directions right, left, up, and down.

This finding is the result of analyzing the distributions of vectors $\frac{\partial L}{\partial \theta_1}$ and $\frac{\partial L}{\partial \theta_2}$ components throughout the training. They point to directions that reduce the error in the optimization space. Components with positive values indicate that the error decreases by moving that binary test to left or up directions and components with negative values indicate that the error decreases by moving that binary test to right or down directions. Components equal to 0 suggest that the error does not change in that direction.

Figure 7 presents the binary tests of an instance patch together with visualizations and distributions of vectors $\frac{\partial L}{\partial \theta_1}$ and $\frac{\partial L}{\partial \theta_2}$ components throughout 30 trai-

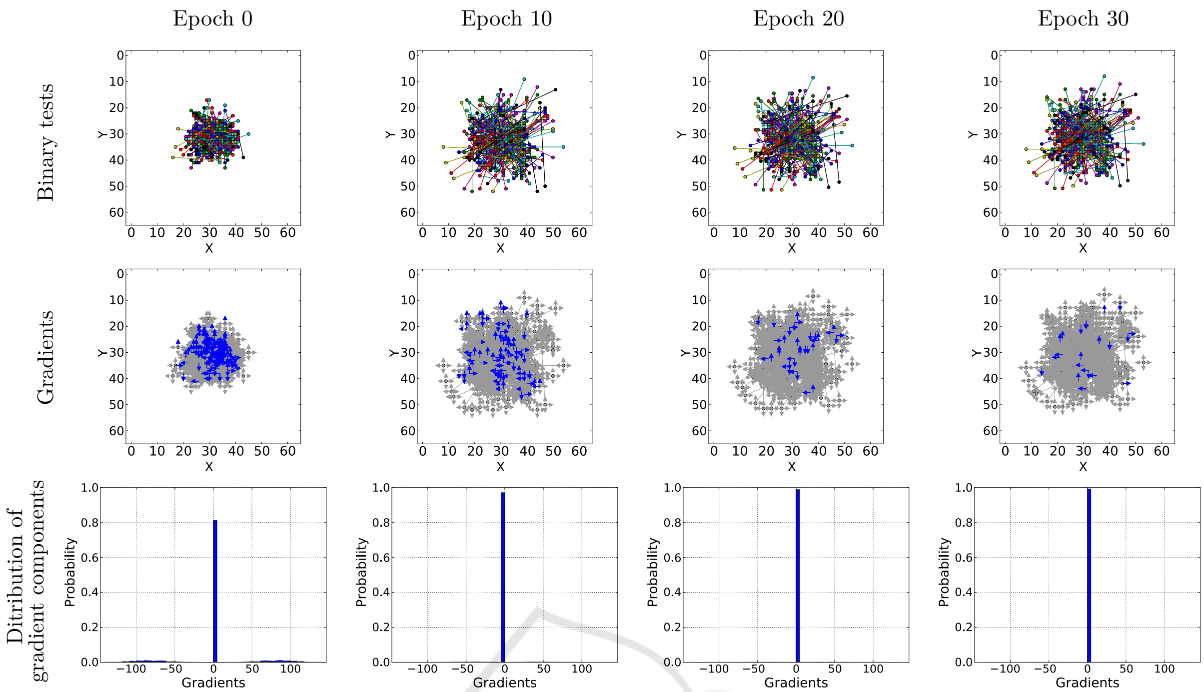

Figure 7: Visualization of gradients $\frac{\partial L}{\partial \theta_i}$ components demonstrating the existence of local minima. The results of Epoch 0 were generated before training starts, with random weights. Images in the top row show the binary tests of an instance patch during training. Images in the mid row show for each selected pixel the directions of its gradients $\frac{\partial L}{\partial \theta_i}$. Blue arrows represent values different from 0 (positive or negative) and indicate the directions to reduce error. Gray arrows represent values equal to 0 and indicate the error keeps the same in those directions and orientations. The bottom row shows the distributions of gradient components, where one can observe the concentration at 0 increases during training, making the network stops learning.

ning epochs. Results of epoch 0 refer to the initial state of the Siamese Network, with weights W_i and b_i randomly initialized, for comparison and analysis. One can see at the first row a spreading of binary tests until the epoch 10 due to the existence of non-zero components (positive or negative) in the gradients, represented by blue arrows at the second image row. Gray arrows represent zero components. Histograms in the third row show a strong concentration of components equal to 0, which means that binary tests will not change anymore and learning has stagnated.

4.3 Impact of Multiscale Trainning

The Local Minimum problem appears because the selection of binary tests was made by analyzing only immediate neighbors of current pixels. This localized view hinders the selection of further pixels and stagnates the network learning after a few training epochs.

To reduce impacts of Local Minimum, we propose to use a multi-scale training, changing patches resolutions after some epochs by applying convolutions with Gaussian kernels. All details of this step are presented in Section 3.4.

Spatial resolution 8×8 was simulated convolving all patches with a Gaussian kernel $G(x, y; k = 25, \sigma = 10)$ and dividing them in a regular grid 8×8 formed by cells of size 8×8 pixels. Resolution 16×16 was simulated with a Gaussian kernel $G(x, y; k = 13, \sigma = 5,2)$ and a grid 16×16 formed by cells of size 4×4 pixels. We also simulated resolution 32×32 with a Gaussian kernel $G(x, y; k = 7, \sigma = 2,8)$ and a grid 32×32 of size 2×2 pixels.

By constraining the selection on central pixels of each grid cell, at respective resolution, binary tests became more spread than initial version of training, as shown in Figure 8. In the first row we show an instance patch varying scale every 10 epochs, starting from resolution 8×8, to 16×16, then 32×32 and finally 64×64 (the original resolution). In the second row we show the binary tests for the displayed patch, where one can observe the regularity of the selected pixels over the grid. At the third row, we show the gradients (colored arrows) of binary tests in its specific resolution. Blue arrows indicate non-zero components while gray arrows indicate components equal to 0. Finally, the fourth row presents the gradient components distributions.

Comparing the gradients and histograms in Figures 7 and 8, one can observe a significant reduction of

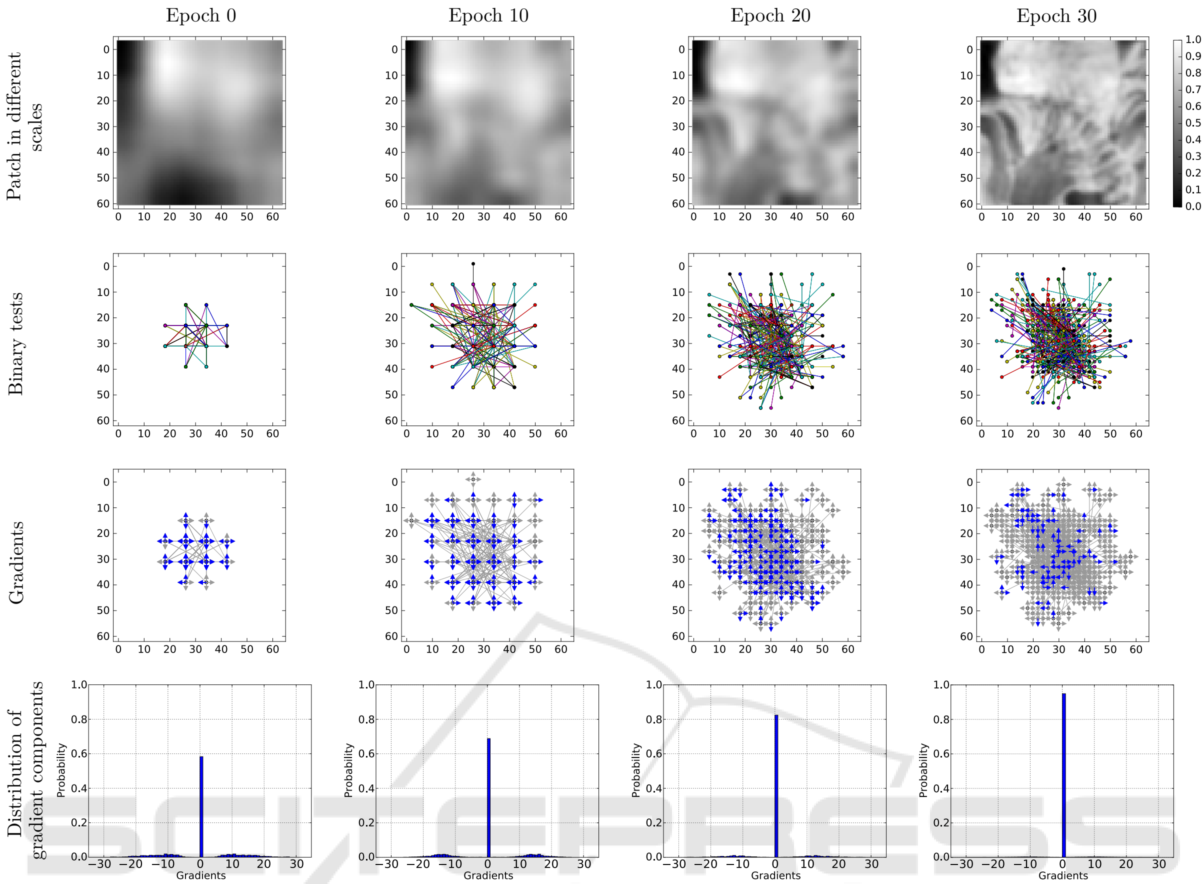

Figure 8: Visualization of gradients $\frac{\partial L}{\partial \theta_i}$ components in multi-scale training illustrating the reduction of Local Minima. Epoch 0 results were generated before any training, with random weights, for comparison purposes. Figures in the first row show an instance patch varying scale during training. The second row shows the binary tests learned for the patch shown above. Third-row show for each selected pixel the directions of its gradients. Blue arrows represent values different from 0 (positive or negative) and indicate the directions to reduce error. Gray arrows represent values equal to 0 and indicate the error keeps the same in those directions and orientations. The last row shows the distributions of gradient components, where one can observe the concentration in 0 was reduced compared of Figure 7.

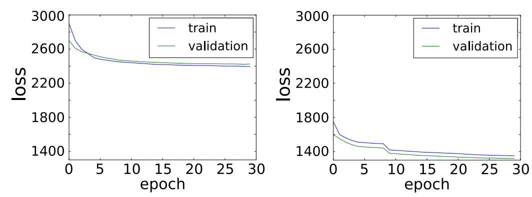

(a) (b)

Figure 9: Error histories in different binary tests learning experiments. a) Trained with patches in the original 64×64 scale. b) Trained with 8×8 scale until epoch 10, then changed to 16×16 scale, learning rate 1×10^{-9}. It is possible to observe a significant decreasing in the loss value, especially when the scale is changed, which demonstrates that the proposed approach was able to lessen the Local Minima problem.

zero components since the beginning of training. That means the Siamese Network found more pixels to reduce the error. At epoch 0 of Figure 7 there were more than 80% of gradient components equal to 0 while Figure 8 shows less than 60% at the same time. On epoch 10 of Figure 7 components equal to 0 exceeded 90% whereas at the same time in Figure 8 this concentration was still less than 70%.

The multiscale trainning allows the network to expand on the covered area over all patches, making possible to select further pixels to form binary tests. We obtained the best result by starting the training patches at spatial resolution 8×8 and, after 10 epochs, changing to resolution 16×16. Figure 9 shows the error curves for the train and validation, comparing standard and multiscale training. Figure 9-a shows that the error started close to $2,900$ at epoch 0 and stabilized around $2,400$ after 30 epochs. Figure 9-b shows that the error started close to $1,700$ and became close to $1,300$ after 30 epochs. From these results we draw the following observation: the proposed appro-

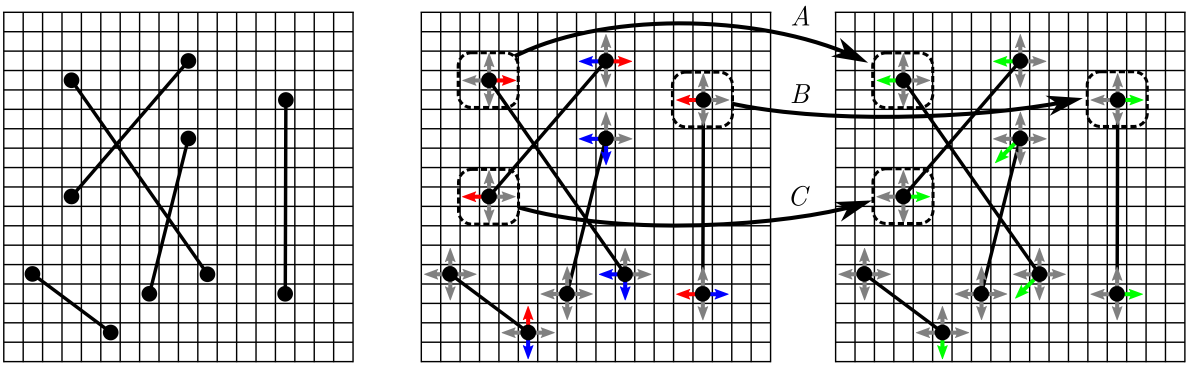

(a) (b) (c)

Figure 10: Illustration of the Incorrect Gradient Components problem. a) Some fictitious binary tests selected during the training. b) Visualization of gradients $\frac{\partial L}{\partial \theta_i}$ components. Arrows represent the loss values behavior given a coordinates θ_i variation of the binary tests in either vertical or horizontal axes. *Blue* indicates a decrease of the loss value in that direction, *red* indicates an increase of the loss value and *gray* indicates no change of the loss value. c) *Green* arrows indicate the resulting directions that should be followed by the Siamese Network weight update. Vectors A, B, and C are the *Incorrect Gradient Components*, since their directions do not decrease the loss value. They are obtained from individual components that either increase or do not modify the loss value.

ach has reduced the impact of Local Minimum, although it was not completely solved.

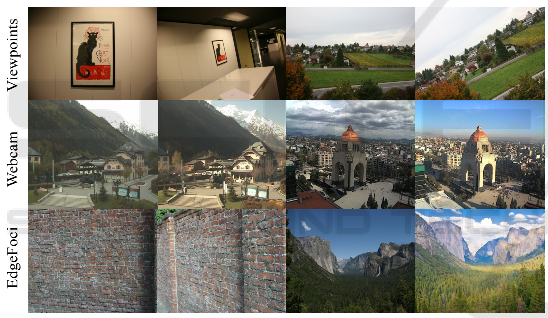

Figure 11: Sample images from Viewpoints (Yi et al., 2016), Webcam (Yi et al., 2016) and EdgeFoci (Ramnath and Zitnick, 2011) datasets.

4.4 Incorrect Gradient Components

The selection of the binary tests based on the immediate pixels neighbors also presents a problem related to some components of the gradient vectors $\frac{\partial L}{\partial \theta_1}$ and $\frac{\partial L}{\partial \theta_2}$. The gradient vector $\nabla f(x)$ indicates the direction and orientation of the greatest rate of increase of the function $f(x)$ from x. To minimize $f(x)$, the Gradient Descent algorithm updates weights W_i and b_i following the gradient direction but in the opposite orientation, what is valid when $f(x)$ is a convex function and the opposite orientation to greatest rate of increase is precisely the one that gives the largest decreasing rate of $f(x)$ at x. We discovered it is not true for the binary tests selection problem.

We also have found that the Siamese Network changes the coordinates of some binary tests not because the neighbor might reduced the error, but simply because the gradients $\frac{\partial L}{\partial \theta_1}$ and $\frac{\partial L}{\partial \theta_2}$ indicate that the function $L(H,y)$ grew up in the opposite orientation. This problem of the learning going to the wrong way to minimize the loss function we called *Incorrect Components of Gradient Problem*.

The gradient $\frac{\partial L}{\partial \theta_1}$ has incorrect components when the inequalities

$$L_1^+ \geq L(H(d_1(x_1,\theta_1),d_2(x_2,\theta_2)),y) \text{ and } \tag{15}$$

$$L_1^- \geq L(H(d_1(x_1,\theta_1),d_2(x_2,\theta_2)),y) \tag{16}$$

are true simultaneously. Similarly, the gradient $\frac{\partial L}{\partial \theta_2}$ contains incorrect components when

$$L_2^+ \geq L(H(d_1(x_1,\theta_1),d_2(x_2,\theta_2)),y) \text{ and } \tag{17}$$

$$L_2^- \geq L(H(d_1(x_1,\theta_1),d_2(x_2,\theta_2)),y). \tag{18}$$

The terms L_1^+, L_1^-, L_2^+ and L_2^- are defined in Eq. 6, 7, 8 and 9. Figure 10 illustrates the components of the gradients $\frac{\partial L}{\partial \theta_1}$ and $\frac{\partial L}{\partial \theta_2}$ for a fictional patch 18×18, where it is possible to visualize the resulting vectors used by the Siamese Network to update the weights W_i and b_i.

4.5 Descriptor Evaluation

To evaluate the proposed binary tests selection methodology, we performed keypoint matchings experiments using images of the datasets Viewpoints (Yi

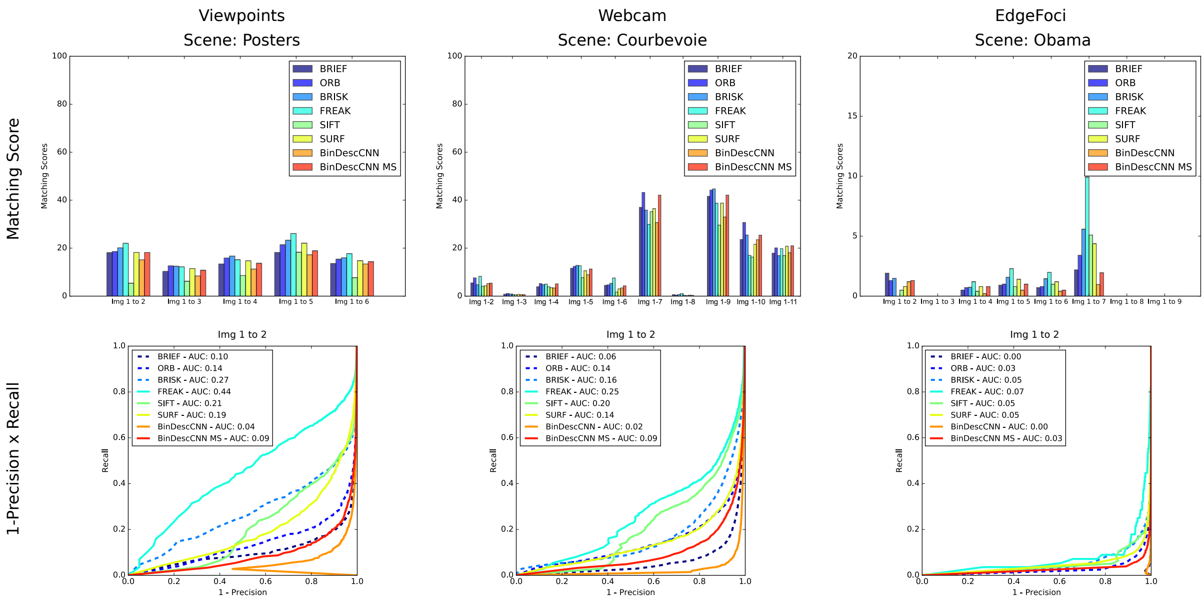

Figure 12: Qualitative evaluation of binary tests learned by the Siamese Network. *BinDescCNN* descriptor represents our model trained on Trevi Fountain dataset with patches in original scale 64×64 while *BinDescCNN MS* were trained with patches in scales 8×8 and 16×16.

et al., 2016), Webcam (Yi et al., 2016), and EdgeFoci (Ramnath and Zitnick, 2011). Each dataset is composed of different images of several scenes. Figure 11 shows some samples of images from the datasets.

Dataset Viewpoints is composed of 30 images in total, divided into 5 different sequences. Each sequence was created from images captured with pose variations. Some of these images have also scale variations. Dataset EdgeFoci contains 38 images divided into 5 sequences with different poses and lighting variations. Webcam has 120 images divided into 6 sequences with lighting variations. The images were acquired with the camera in a fixed position throughout the day in different seasons.

We first evaluate the quality of the descriptor in a matching task. We used a *Matching Score* defined as the fraction of correctly matched keypoints between two images. We evaluated two models: *BinDescCNN* that was trained with patches of the dataset Trevi Fountain in original resolution 64×64; and the *BinDescCNN MS* that was trained with multi-scale patches, as described in subsection 3.4. The *BinDescCNN MS* model presented better results than *BinDescCNN* due to a reduction of Local Minimum impacts, which allowed a better choice of pixels to compose binary tests. We compared our results against the floating point descriptors SIFT and SURF and also the known binary descriptors BRIEF, ORB, BRISK and FREAK. To avoid any bias, all descriptors were evaluated using the ORB algorithm as a keypoint detector.

We also used the *Area Under the Curve* (AUC) of *1-Precision* $\times$ *Recall* chart. *Precision* is a measure of the probability that a sample is correctly classified when a model says it belongs to a certain class. *Recall* evaluates how many correct samples have been classified as correct. Figure 12 shows some results obtained on datasets Viewpoints, Webcam and EdgeFoci, respectively. In general, our models reached a *Matching Score* close to the BRIEF and ORB descriptors, but worse than BRISK, FREAK, and SURF. In this same metric, the SIFT descriptor performance was poorer than others due to use of ORB as keypoint detector. We believe that the detected keypoints are not appropriate to SIFT because their gradients distributions are not discriminative enough. Results presented in the curves *1-Precision* $\times$ *Recall* show that, in general, our descriptor is better than BRIEF, however demonstrated some confusion when performing matchings. Despite the reasonable amount of correct matchings our approach still produces large number of False Positives and False Negatives.

5 CONCLUSION

In this work, we show that binary tests learned by the Siamese Network are still a major challenging task for CNN. Network's learning stops after a few epochs due to the *Local Minima* and *Incorrect Gradient Components* problems, what make difficult to separate corresponding and non-corresponding patches properly. We conclude that not always a CNN based model will be able to find a spatial binary tests distribution to minimize the distances between corresponding keypoints and maximize the distances between non-corresponding keypoints. The results presented do not prove the impossibility of using Convolutional Neural Networks to select binary tests, but they clarify some limitations when using the local pixel's neighborhood.

ACKNOWLEDGEMENTS

The authors would like to thank the agencies CAPES, CNPq, and FAPEMIG for funding different parts of this work.

REFERENCES

Balntas, V., Tang, L., and Mikolajczyk, K. (2015). Bold - binary online learned descriptor for efficient image matching. In *The IEEE Conference on Computer Vision and Pattern Recognition (CVPR)*.

Bay, H., Tuytelaars, T., and Gool, L. V. (2006). Surf: Speeded up robust features. In *In ECCV*, pages 404–417.

Calonder, M., Lepetit, V., Strecha, C., and Fua, P. (2010). Brief: Binary robust independent elementary features. In *Proceedings of the 11th European Conference on Computer Vision*, pages 778–792.

Chollet, F. et al. (2015). Keras.

Dalal, N. and Triggs, B. (2005). Histograms of oriented gradients for human detection. In *Proceedings of the 2005 IEEE Computer Society Conference on Computer Vision and Pattern Recognition (CVPR'05) - Volume 1 - Volume 01*, pages 886–893.

Duan, Y., Lu, J., Wang, Z., Feng, J., and Zhou, J. (2017). Learning deep binary descriptor with multi-quantization. In *The IEEE Conference on Computer Vision and Pattern Recognition (CVPR)*.

Leutenegger, S., Chli, M., and Siegwart, R. Y. (2011). Brisk: Binary robust invariant scalable keypoints. In *Proceedings of the 2011 International Conference on Computer Vision*, pages 2548–2555.

Lin, K., Lu, J., Chen, C.-S., and Zhou, J. (2016). Learning compact binary descriptors with unsupervised deep neural networks. In *IEEE Conference on Computer Vision and Pattern Recognition (CVPR)*.

Lowe, D. G. (2004). Distinctive image features from scale-invariant keypoints. *Int. J. Comput. Vision*, pages 91–110.

Ortiz, R. (2012). Freak: Fast retina keypoint. In *Proceedings of the 2012 IEEE Conference on Computer Vision and Pattern Recognition (CVPR)*, pages 510–517.

Ramnath, K. and Zitnick, C. L. (2011). Edge foci interest points. In *2011 IEEE International Conference on Computer Vision (ICCV 2011)(ICCV)*, pages 359–366.

Rublee, E., Rabaud, V., Konolige, K., and Bradski, G. (2011). Orb: An efficient alternative to sift or surf. In *Proceedings of the 2011 International Conference on Computer Vision*, pages 2564–2571.

Simo-Serra, E., Trulls, E., Ferraz, L., Kokkinos, I., Fua, P., and Moreno-Noguer, F. (2015). Discriminative learning of deep convolutional feature point descriptors. In *2015 IEEE International Conference on Computer Vision (ICCV)*, pages 118–126.

Simonyan, K. and Zisserman, A. (2015). Very deep convolutional networks for large-scale image recognition. In *In Proc. of International Conference on Learning Representations (ICLR)*.

Theano Development Team (2016). Theano: A Python framework for fast computation of mathematical expressions.

Winder, S. and Brown, M. (2007). Learning local image descriptors. In *Proceedings of the International Conference on Computer Vision and Pattern Recognition (CVPR07)*.

Xu, X., Tian, L., Feng, J., and Zhou, J. (2014). OSRI: A rotationally invariant binary descriptor. *IEEE Trans. Image Processing*, pages 2983–2995.

Yi, K. M., Verdie, Y., Fua, P., and Lepetit, V. (2016). Learning to Assign Orientations to Feature Points. In *Proceedings of the Computer Vision and Pattern Recognition*.